Journal of Petroleum
Science and Technology

Single Step and Non-Catalytic Process for Formaldehyde Production from Methane using Microchannel Reactor: Theoretical Analysis

Hamid Abbasi, Fariborz Rashidi*, and Mohammad Mahdi Moshrefi

Department of Chemical Engineering, Amirkabir University of Technology, Tehran, Iran

ABSTRACT

Conventionally, methane is reformed into syngas, and subsequently converted into C_1-oxygenates (methanol and formaldehyde). A novel option is the catalyst-free single-step conversion of methane to C_1-oxygenates. This study presents a comprehensive model of methane partial oxidation to formaldehyde as an intermediate chemical species in methane oxidation process using microreactor. The dependency of C_1-oxygenates yield on operating parameters is crucial. Therefore a representative mathematical model is constructed and solved in order to investigate the effect of operating temperature, feed flow-rate, and composition on the formaldehyde yield. Fifty-four coupled of differential equations are solved by finite element method. Moreover, to simulate the process, GRI-Mech 3.0 is employed as the reaction kinetics. A good agreement was achieved when the model results were compared with experimental data from the literature in terms of formaldehyde concentration and methane conversion. Finally, results of the study are presented and discussed on the basis of a major reaction pathway proposed in this study for methane oxidation at low temperature, and the important design criteria are presented. With respect to the model results, 5.5% yield for formaldehyde per one pass of microreactor was achieved at the operating condition of T = 1000 K and O_2/CH_4 ratio = 17.

Keywords: Methane, Formaldehyde, Microreactor, Single Step, Non-catalytic, Kinetic Study.

INTRODUCTION

Conversion of natural gas into valuable chemicals and easily transportable liquid fuels is the focus of interest. This is due to the fact that methane as the main component of natural gas plays an important role in the petrochemical industry. C_1-oxygenates are considered either an important source of petrochemicals or as intermediates. Moreover, the conventional processes for conversion of methane to C_1-oxygenates suffer from high-maintenance catalyst demand. It requires massive scale plants in order to be economically profitable, while there are numerous natural gas sources with low capacity to become a candidate for syngas technologies [1]. Methane could be converted into C_1-oxygenates via two routes: either by forming syngas from steam reforming followed by catalytic conversion at high pressure or by direct conversion methods

***Corresponding author**
Fariborz Rashidi
Email: rashidi@aut.ac.ir
Tel: +98 21 64540
Fax: +98 21 6454 3190

Article history
Received: January 27, 2019
Received in revised form: May 08, 2019
Accepted: May 13, 2019
Available online: August 7, 2019
DOI: 10.22078/jpst.2019.3626.1576

using partial oxidation [1]. Almost all commercial processes for large scale natural gas conversion involve syngas step [2-5]. However, these massive processes are energy intensive due to the necessity of syngas production step [6], high-maintenance catalysts, and operating conditions of high pressures (200-600 psi) [1,7]. Consequently, these processes suffer from low energy efficiency and high capital and operating costs [8]. It is noted that more than 60% of the capital cost for the indirect process is associated with converting methane to syngas [9].

Therefore, direct partial oxidation of methane to C_1-oxygenates might be a promising alternative for effective use of abundant natural gas resources [2,10]. Moreover, direct routes have the potential of economic advantage over indirect method [1] They may be a breakthrough for the utilization of methane into useful chemicals. Both homogeneous gas phase reactions, e.g. [11-13] and heterogeneous catalytic reactions, e.g. [14-21] have been comprehensively investigated. It seems that the main challenge for direct routes is selectivity improvement without reducing conversion per single pass [22]. Direct partial oxidation of methane to C_1-oxygenates has also been studied by other methods such as biocatalysis [23,24], membrane technology [25, 26], photocatalysts technology [27], and etc. A techno-economical assessment showed that direct process for C_1-oxygenates production could compete with conventional indirect one in terms of production costs if 80% selectivity of methanol could be achieved at single pass methane conversion of 10% [8].

Hence all these methods suffer from the low yield of C_1-oxygenates, and the reported yields are still not high enough to compete with the current multi-step process [6]. But this is not the end and in fact, microreactors due to low residence time, high heat, and mass transfer rates, low-pressure drop, uniform temperature distribution, and high surface to volume ratio provide a window of opportunity regarding direct synthesis route [28-32]. C_1-oxygenates are intermediates in chain reactions of methane partial oxidation, and objective should be to stop the progression of the reaction channel of $CH_4 \rightarrow CH_3 \rightarrow CH_2O \rightarrow HCO \rightarrow CO \rightarrow CO_2$ when the formaldehyde reaches the maximum amounts. Achieveing that goal requires strict control on residence time. Furthermore, rapid heat quenching should be realized which might be possible by the employment of microreactors [31].

Due to high surface per volume ratio, the microreactors may have a high heat transfer rate about 106 K/s [33]. In general, control of methane partial oxidation operation under free radical mechanism is a serious concern [1]. The dependency of C_1-oxygenates yield on various parameters is crucial. Moreover, a representative mathematical model is constructed and solved in order to get a deep understanding of catalyst-free single step methane conversion into C_1-oxygenates by microreactors. The kinetic mechanism of GRI-Mech 3.0 which is optimized for a wide range of thermodynamic conditions (1000K to 2500K, 10 Torr to 10 atm) and equivalence ratios (0.1 to 5) [34] have been chosen as reaction kinetic. The developed mathematical model has been solved numerically by the finite element method (FEM) using COMSOL Multiphysics 5.3a.

EXPERIMENTAL PROCEDURE

Model Description

Model construction is based on general property balance equations which mathematically describe transport phenomena. Mass, momentum, and

energy are the three phenomena that their conservation equations finally lead to a set of non-linear partial differential equations. In Figure 1, the proposed schematic diagram for an annular flow microreactor system configuration is shown. It is assumed that perfectly, premixed ideal gases of argon, methane, and oxygen are fed into the microreactor system at a steady state condition.

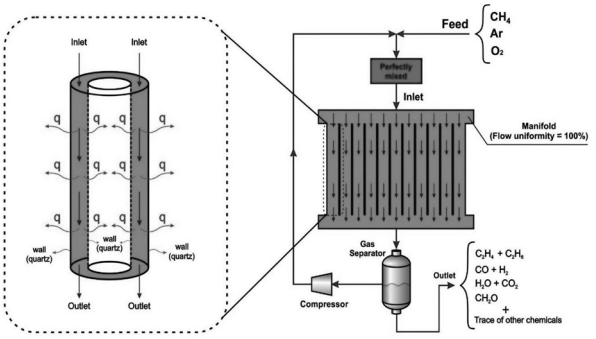

Figure 1: Schematic diagram of annular flow micro reactor configuration.

Although the microreactor system consists of a set of parallel channels, only one channel is modeled assuming flow is uniformly distributed in all channels [35,36]. Equation 1-a defines the mass balance equation for the annular flow microreactor [37]:

$$\frac{\partial C_i}{\partial t} + \nabla.(-D_i \nabla C_i) + U.\nabla C_i = R_i \qquad (1-a)$$

The dimensionless form of Equation (1-a) is depicted in Equation 1-b [38].

$$\left(\frac{\partial C^*}{\partial t} + U.\frac{\partial C^*}{\partial \lambda}\right) = \frac{1}{Pe_{MT}}\left(\frac{\partial^2 C^*}{\partial \lambda^2} + \sum_j \upsilon_{ij}\Lambda_{ij}^2 R_j^*\right) \qquad (1\text{-b})$$

$$C^* = \frac{C_i}{C_{i0}},\ \lambda = \frac{z}{L},\ \frac{k_j(T)L^2(C_{i0})^{n_j-1}}{D} = \Lambda_{ij}^2,\ Re.Sc = Pe_{MT}.$$

The Reynolds number in the annular microreactor is found to be lower than 150 in reacting conditions [33]. High axial Peclet number (Pe_{MT}) (higher than 300) [6,33] suggests that in the mass balance equation, advection term play a dominant role over diffusion term. Also, radius dependency of concentration could be ignored since L/D ratio is too large. In addition, the volumetric flow rate in microreactor is assumed constant since the output flow rate is almost equal to the input flow rate due to highly diluted reactants (90% Argon).

Eventually, the mass balance equation for the annular flow microreactor is reduced to Equation 2:

$$\frac{dF_i}{dV} = R_i \text{ or } \frac{dC_i}{d\tau} = R_i,\ R_i = \sum_{j=1}^{325}\upsilon_{ij} r_j,\ i = 1:53, \text{ chemical species}$$
$$\text{and } j = 1:325, \text{ reversible reactions} \qquad (2)$$

which i stands for O, O_2, H, OH, H_2, HO_2, H_2O_2, CH, CO, CH_2, HCO, CH_2(s), CH_3, CH_2O, CH_4, CO_2, CH_2OH, CH_3O, CH_3OH, C_2H, C_2H_2, HCCO, C_2H_3, CH_2CO, C_2H_4, C_2H_5, C_2H_6, H_2O, N_2, Ar, C, HCCOH, N, NO, N_2O, NO_2, NH, HNO, NH_2, NNH, CN, NCO, HCN, HOCN, HNCO, H_2CN, HCNN, HCNO, NH_3, CH_2CHO, CH_3CHO, C_3H_8, and C_3H_7.

Reaction term in mass balance equation is based on the GRI-Mech 3.0 which consists of 53 species and 325 elementary reactions [34]. It is necessary to solve mass and heat transfer equations simultaneously. The energy balance equation for annular flow microreactor system is written as Equation 3 [37]:

$$A_c \times \rho \times C_{p,i}\frac{\partial T}{\partial t} + A_c \times \rho \times C_{p,i} \times u.\nabla T + \nabla.q_{cond} =$$
$$A_c \times Q + A_c \times Q_{ext},\ q_{cond} = -A_c \times k \times \nabla T \qquad (3)$$

Similar to mass balance equation circumstance, after some straightforward manipulations, Equation 3 is decreased to Equation 4.

$$\sum_{i=1}^{325} F_i \times C_{p,i} \times \frac{dT}{dV} = Q_{heat\ source} + Q_{ext},\ Q_{heat\ source} = -\sum_{j=1}^{325} H_j r_j \qquad (4)$$

The derived Equations 2 and 4 with their related boundary conditions in Table 1 were solved by the FEM using COMSOL Multiphysics 5.3a. The specific mesh size of the microreactor (about 3500 elements) with an extremely fine grid near the inlet

and outlet and the 10000 fixed number of elements in the domain of the annular microreactor was developed. In addition, simulations were carried out in order to make the element size independent from the solution.

Table 1: Boundary types and conditions of the microchannel in the microreactor system.

Boundary type	Boundary condition
Inlet	$C = C_i^{in}(\frac{O_2}{CH_4} = 0.4 - 20 \text{ and } x_{O_2} + x_{CH_4} = 0.1)$, $T = T^{in}(T^{in} = 1000,1050,1100,1150,1250)$, $P = 2\,bar$
Outlet	$\frac{dc_i}{dz} = 0,\ \frac{dT}{dz} = 0,\ P = 2\,bar$
Wall	$n.N_i = 0,\ n.q = 0,$ No surface reactions

Reaction Pathways Analysis

The major reaction pathways for low-temperature oxidation (LTO) of methane are illustrated in Figure 2. The elementary reactions considered in pathways are based on those introduced by Glarborg et al [39] and reaction kinetic of GRI-Mech 3.0. An important point regarding Figure 2 is the width of the arrows which refer to the relative importance of each particular reaction path. For simplicity, pathways with reaction rate of less than 1.00E-7 gmol/cm/s are not shown. Reaction kinetics of pathways which have a higher order of importance with their related Arrhenius parameters are presented in Table 2 [34].

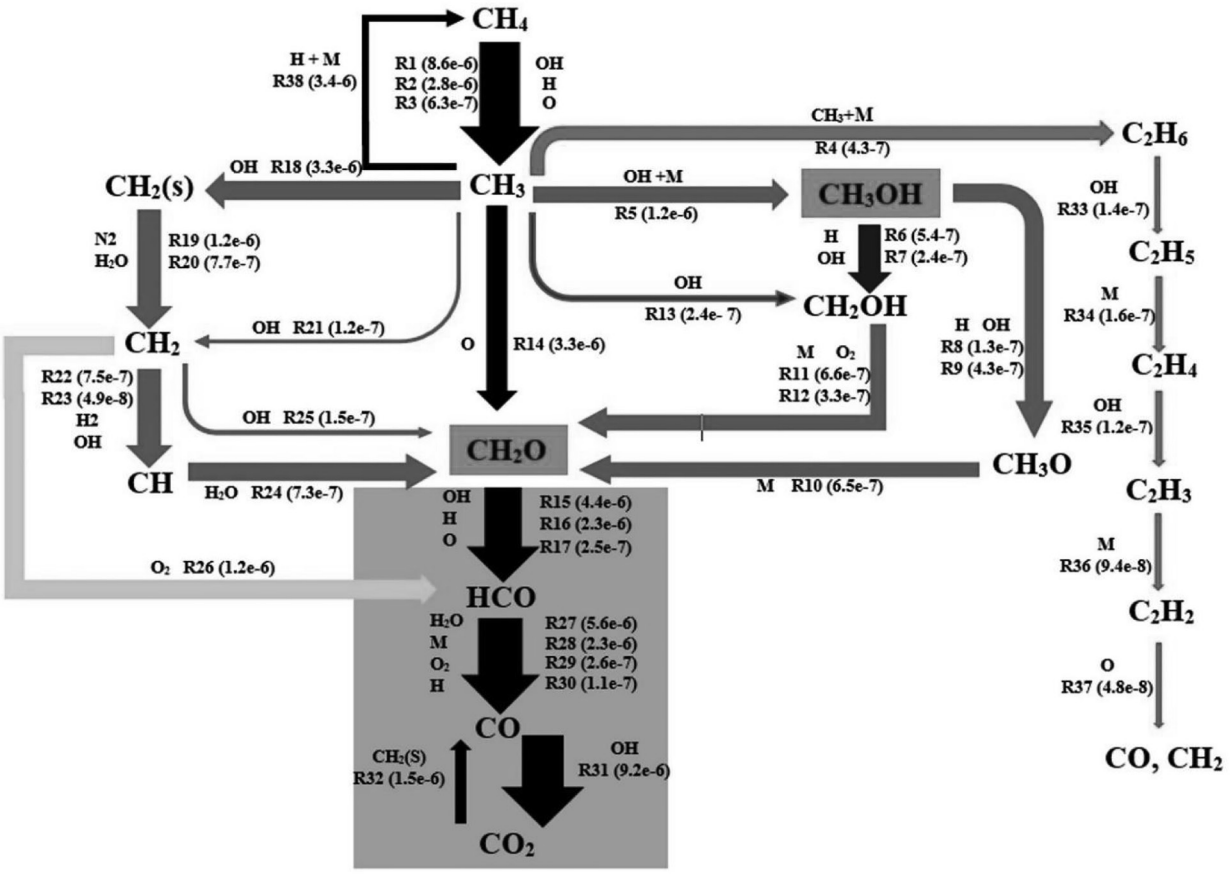

Figure 2: Major reaction pathways diagram according to GRI-Mech 3.0 for low temperature oxidation of methane, reaction rates are shown in parenthesis.

Table 2: Elementary reactions with Arrhenius parameters corresponding to reaction pathways (Figure 2) [40].

Number	Reaction	Forward rate coefficient[1]		
		A	n	E
1	$OH + CH_4 = CH_3 + H_2O$	100	1.6	13054.08
2	$H + CH_4 = CH_3 + H_2$	660.0	1.62	45354.560
3	$O + CH_4 = OH + CH_3$	1020.0	1.5	35982.40
4	$CH_3 + CH_3 (+M) = C_2H_6 (+M)$	6.77 E+10	-1.18	2736.33
5	$OH + CH_3 (+M) = CH_3OH (+M)$	2.79 E+12	-1.43	5564.72
6	$H + CH_3OH = CH_2OH + H_2$	17.00	2.1	20376.08
7	$OH + CH_3OH = CH_2OH + H_2O$	1.44	2.0	-3514.56
8	$H + CH_3OH = CH_3O + H_2$	4.20	2.1	20376.08
9	$OH + CH_3OH = CH_3O + H_2O$	6.30	2.0	6276.0
10	$H + CH_2O (+M) = CH_3O (+M)$	5.40 E+5	0.454	10878.40
11	$H + CH_2O (+M) = CH_2OH (+M)$	5.4 E+5	0.454	15062.40
12	$CH_2OH + O_2 = HO_2 + CH_2O$	1.80 E+7	0.0	3765.60
13	$H + CH_2OH = OH + CH_3$	1.60E+5	0.65	-1188.256
14	$O + CH_3 = H + CH_2O$	5.06 E+7	0.0	0.0
15	$OH + CH_2O = HCO + H_2O$	3430.0	1.18	-1870.248
16	$H + CH_2O = HCO + H_2$	57.40	1.90	11472.528
17	$O + CH_2O = OH + HCO$	3.90 E+7	0.0	14811.36
18	$OH + CH_3 = CH_2(s) + H_2O$	6.44 E+11	-1.34	5928.728
19	$CH_2(s) + N_2 = CH_2 + N_2$	1.50E+7	0.0	2510.4
20	$CH_2(s) + H_2O = CH_2 + H_2O$	3.00E+7	0.0	0.0
21	$OH + CH_3 = CH_2 + H_2O$	56.0	1.6	22677.28
22	$CH + H_2 = H + CH_2$	1.08E+8	0.0	13012.24
23	$OH + CH_2 = CH + H_2O$	1.13E+7	2.0	3000
24	$CH + H_2O = H + CH_2O$	5.71E+6	0.0	-3158.92
25	$OH + CH_2 = H + CH_2O$	11.30	2.0	12552.0
26	$CH_2 + O_2 = OH + HCO$	5.0E+7	0.0	6276.0
27	$HCO + H_2O = H + CO + H_2O$	1.5E+12	-1.0	71128.0
28	$HCO + M = H + CO + M$	1.87E+11	-1.0	71128.0
29	$HCO + O_2 = HO_2 + CO$	1.345E+7	0.0	1673.60
30	$H + HCO = H_2 + CO$	7.34E+7	0.0	0.0
31	$OH + CO = H + CO_2$	47.60	1.228	292.88
32	$CH_2(s) + CO_2 = CO + CH_2O$	1.40E+13	0.0	0.0
33	$OH + C_2H_6 = C_2H_5 + H_2O$	3.54	2.12	3640.08
34	$H + C_2H_4 (+M) = C_2H_5 (+M)$	5.40E+5	0.454	7614.88
35	$OH + C_2H_4 = C_2H_3 + H_2O$	3.60	2.0	1460.0
36	$H + C_2H_2 (+M) = C_2H_3 (+M)$	56.00E+5	0.0	10041.60
37	$O + C_2H_2 = CO + CH_2$	6.94	2.0	7949.6
38	$H + CH_3 (+M) = CH_4 (+M)$	1.39E10	-0.534	2242.624

[1]The forward rate coefficient $k = A*(T/T_{ref})^n \exp(-E/R/T)$. R is universal gas constant (J/mol/K), T is the temperature in K, and T_{ref} equals 1 K. the units of A involve mol/cm^3 and s, E is J/mol.

The linear progression of CH_4 to CO_2, together with several side loops originating from methyl radical is shown in reaction pathways. Moreover, the starting point of CH_4 linear progression (Black) is from reactions where OH, H, and O radicals attack CH_4 to produce CH_3. Methyl radical then combines with an oxygen atom to form formaldehyde (target product of this study). Subsequently, formaldehyde reacts with OH, H, and O radicals to form formyl radical (HCO). Follow-up formyl radical is transformed to CO through four elementary reactions, and finally, CO is converted to CO_2.

In addition to the direct pathway of methyl radical to formaldehyde, there also exist side loops (Blue) where they all end up in formaldehyde formation except one (Orange). Meanwhile, C_2 hydrocarbons originated from CH_3 end up forming CO (and CH_2) (Red). Consequently, in order to have formaldehyde as the target product, side loop (Orange), C_2 hydrocarbons (Red), and linear progression of formaldehyde to CO and CO_2 ($CH_2O \rightarrow CO \rightarrow CO_2$, which is highlighted at reactions pathways by gray) must be prevented.

RESULTS AND DISCUSSION

Methanol and formaldehyde are among intermediates in the oxidation of methane. C–H bond in methane is stronger than that of C_1-oxygenates, and therefore extraction of C_1-oxygenates from the reaction zone is challenging as they are more reactive than methane itself [41]. Hence the main concern is how to achieve a high order of C_1-oxygenates selectivity at acceptable methane conversions [2,8]. According to the published literature, in the LTO of methane ($T < 1500$ K and $1 < P < 10$ bar), production of methanol is much lower than formaldehyde [42]. Moreover, in this study formaldehyde is representative of C_1-oxygenates. As mentioned earlier, microreactor might be an appropriate apparatus for LTO of methane to produce formaldehyde. Being an intermediate in the process of methane oxidation, the objective would be to withdraw formaldehyde as the product from the output of microreactor before it is converted to other species. In the followings, initially, the mathematical model for the methane oxidation proposed in this study is validated, and then the effect of feed temperature, O_2/CH_4 ratio and residence time which are determining parameters in conversion of methane to formaldehyde are discussed.

Validation

To validate the constructed mathematical model, it is noted that the well-validated reaction kinetic of GRI-Mech 3.0 was used in the mass balance equation. however, the obtained results of the mathematical model were compared with the few experimental results reported by Zhang et al [13]. As reported in Table 3, there is a good agreement between model and experimental results in terms of formaldehyde mole fraction and methane conversion.

Methane Conversion

Methane conversion (Equation 5) at LTO to formaldehyde versus residence time at different temperatures and O_2/CH_4 ratios are illustrated in Figures 3 and 4.

$$\text{Methane conversion} = \frac{\text{moles of methane converted}}{\text{mole of methane introduced}} \times 100 \quad (5)$$

Table 3: Comparison of mathematical model results with experimental results in terms of formaldehyde mole fraction and methane conversion [43].

Number	Operating condition	Formaldehyde mole fraction			Methane conversion (%)		
		Simulation	Experimental	Relative error (%)	Simulation	Experimental	Relative error (%)
1	$O_2/CH_4 = 2$ $T = 1198$ $\tau = 20\,ms$	4.34 E-5	4.18 E-5	3.82	0.15	0.14	7.14
2	$O_2/CH_4 = 2$ $T = 1233$ $\tau = 20\,ms$	7.63 E-5	7.27 E-5	4.95	0.65	0.61	6.55
3	$O_2/CH_4 = 2$ $T = 1273$ $\tau = 20\,ms$	2.05 E-4	1.92 E-4	6.77	2.74	2.71	1.10
4	$O_2/CH_4 = 2$ $T = 1223$ $\tau = 20\,ms$	7.01 E-5	6.78 E-5	3.39	0.44	0.41	7.31
5	$O_2/CH_4 = 2$ $T = 1223$ $\tau = 29.83\,ms$	1.31 E-4	1.28 E-4	2.34	1.71	1.67	2.4
6	$O_2/CH_4 = 2$ $T = 1223$ $\tau = 40\,ms$	2.48 E-4	2.36 E-4	5.08	3.80	3.76	1.06
7	$O_2/CH_4 = 4$ $T = 1223$ $\tau = 20\,ms$	0.90 E-4	8.38E-5	7.39	2.44	2.4	1.67
8	$O_2/CH_4 = 8$ $T = 1223$ $\tau = 20\,ms$	7.89 E-5	7.60 E-5	3.81	6.07	6.0	1.17
9	$O_2/CH_4 = 5$ $T = 1223$ $\tau = 20\,ms$	8.64 E-5	8.22 E-5	5.12	3.18	3.15	0.95
10	$O_2/CH_4 = 2$ $T = 1223$ $\tau = 50\,ms$	1.81e-4	1.70e-4	6.47	4.39	4.37	0.45

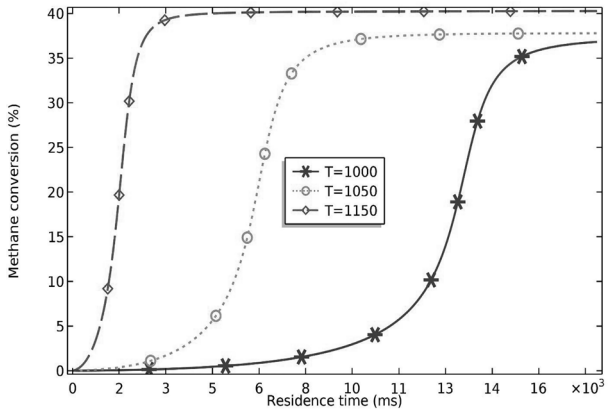

Figure 3: Methane conversion versus residence time at different temperatures. Reaction conditions: P_t = 2 bar, O_2/CH_4 ratio = 0.4 and mole fraction of Argon = 90%.

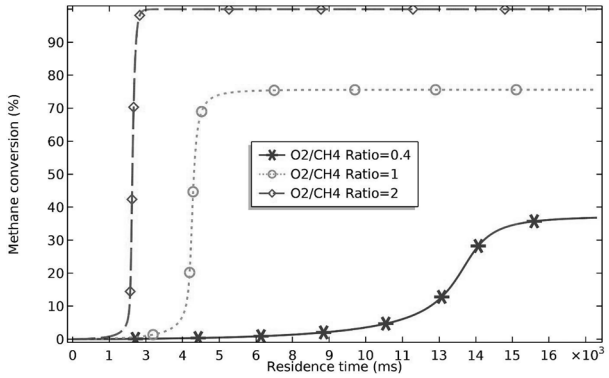

Figure 4: Methane conversion versus residence time at different O_2/CH_4 ratios. Reaction conditions: P_t = 2 bar, T = 1000 K and mole fraction of Argon = 90%.

Variations of methane conversion along the microreactor length with temperature and O_2/CH_4 ratio suggest that methane conversion at LTO reactions could be divided into two zones as

(a)-where methane conversion is very low and only negligible amount of formaldehyde is being formed and (b)-where methane conversion increases rapidly to complete the reaction. This is the crucial zone where formaldehyde production rate (R5, R13, R14, R18, and R21 of reaction pathways) is higher than its consumption rate (R15, R16, and R17 of reaction pathways). Of course, all loops are active as well to produce oxidation products (CO_2 and H_2O). Consequently, in order to achieve a reasonable amount of formaldehyde as a target product in the microreactor the zone (a) and only starting portions of the zone (b) are concentrated.

Formaldehyde Selectivity

In methane LTO process, achieving a high order of selectivity (Equation 6) for the desired product is a crucial challenge. O_2/CH_4 ratio, operating temperature and residence time are the key effective parameters.

$$\text{Formaldehyde selectivity} = \frac{\text{moles of formaldehyde formed}}{\text{mole of methane converted}} \times 100 \quad (6)$$

However, O_2/CH_4 ratio and temperature have a high order of interaction, and therefore their effects are analyzed together. In Figures 5 to 7, formaldehyde selectivity versus residence time at different temperatures and O_2/CH_4 ratios.

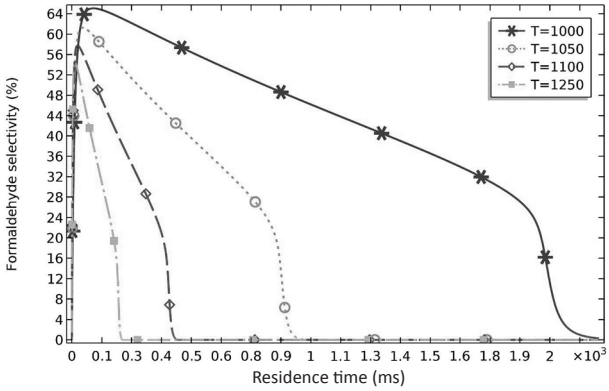

Figure 5: Formaldehyde selectivity versus residence time at different temperatures. Reaction conditions: P_t = 2 bar, O_2/CH_4 ratio = 2 and mole fraction of Argon = 90%.

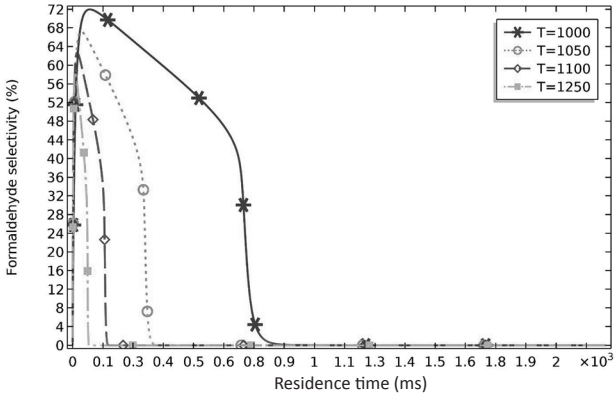

Figure 6: Formaldehyde selectivity versus residence time at different temperatures. Reaction conditions: P_t = 2 bar, O_2/CH_4 ratio = 8 and mole fraction of Argon = 90%.

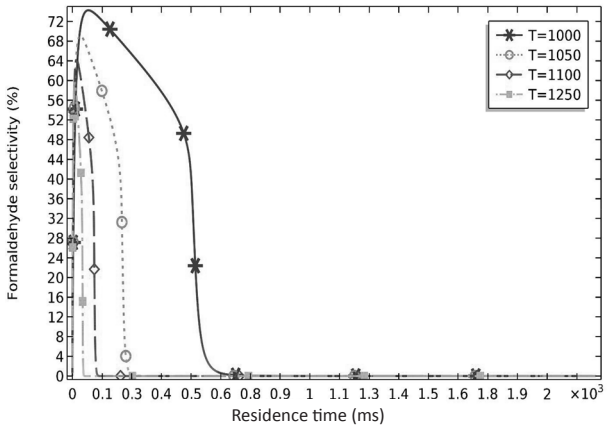

Figure 7: Formaldehyde selectivity versus residence time at different temperatures. Reaction conditions: P_t = 2 bar, O_2/CH_4 ratio = 15 and mole fraction of Argon = 90%.

As shown in Figure 2 and reaction path analysis, the temperature rise has a stronger effect on formaldehyde consumption rate (R15, R16, R17 of reaction pathways) than its production rate (R5, R13, R14, R18, R21 of reaction pathways). This is due to the higher reaction rate constants because of lower activation energies related to formaldehyde consumption reactions. Consequently, the temperature rise will result in a sharper drop of formaldehyde selectivity to zero along reactor length as seen in Figures 5 to 7. In other words, the fall in selectivity happens earlier at the entrance of microreactor as temperature increases. With regard to O_2/CH_4 ratio effect, it is seen that increasing O_2/CH_4 ratio causes a slight increase in the selectivity percent, but again drop of formaldehyde selectivity becomes sharper, and at shorter intervals of reactor inlet, the selectivity of formaldehyde becomes zero.

Formaldehyde Yield

Although single pass formaldehyde selectivity is important, it should be noted that choosing selectivity as a criterion is not practical by itself because methane conversion at maximum selectivity of the formaldehyde is very low (< 1%). Hence, formaldehyde yield (Equation 7) takes into account, and both selectivity and conversion are a more meaningful basis for reactor design.

$$\text{Formaldehyde yield} = \frac{\text{moles of formaldehyde formed}}{\text{mole of methane introduced}} \times 100 = \text{selectivity} \times \text{conversion} \quad (7)$$

As previously seen, formaldehyde selectivity versus residence time has an ascending trend followed by descending trend, while conversion is ascendant in all domains. This causes formaldehyde yield to have a similar trend as its selectivity, which is shown in Figure 8.

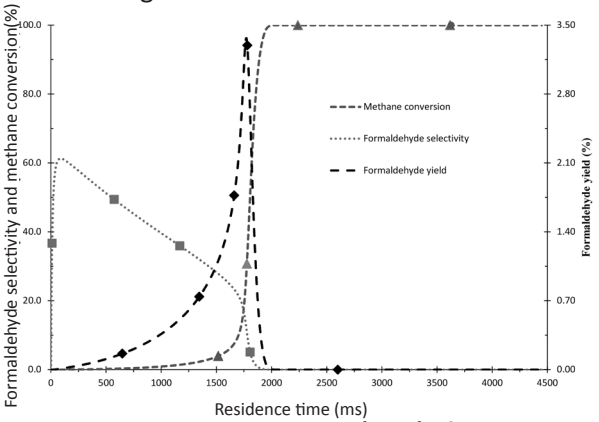

Figure 8: Methane conversion (Blue), formaldehyde selectivity (Red) and yield (Black) versus residence time. Reaction conditions: P_t = 2 bar, O_2/CH_4 = 2, T = 1050 K, and mole fraction of Argon=90%.

Formaldehyde yield versus residence time under different operating temperatures and O_2/CH_4 ratios are presented in Figures 9 to 11.

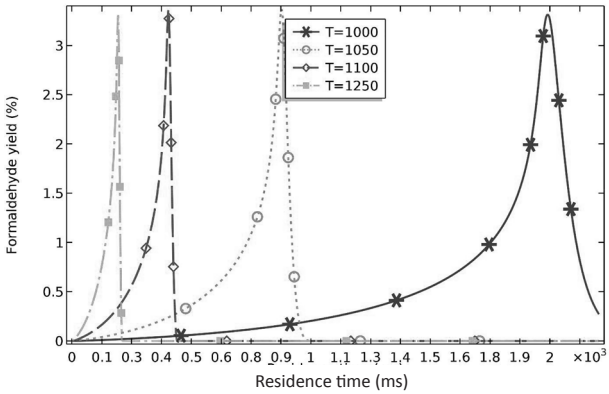

Figure 9: Formaldehyde yield versus residence time at different temperatures. Reaction conditions: P_t = 2 bar, O_2/CH_4 ratio = 2, and mole fraction of Argon = 90%.

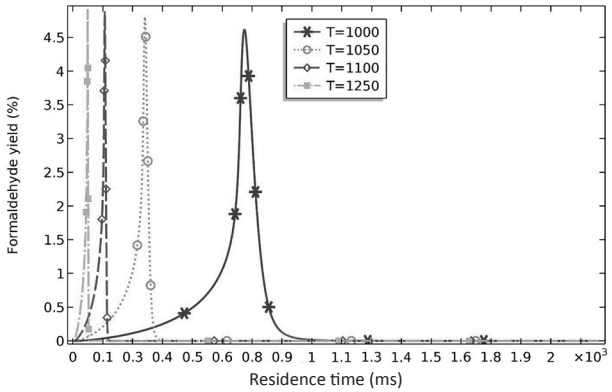

Figure 10: Formaldehyde yield versus residence time at different temperatures. Reaction conditions: P_t = 2 bar, O_2/CH_4 ratio = 8, and mole fraction of Argon = 90%.

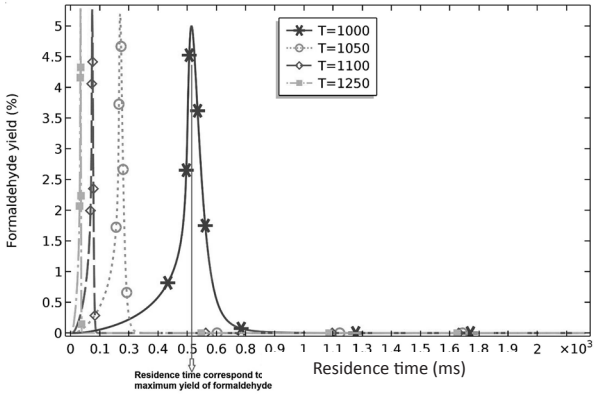

Figure 11: Formaldehyde selectivity versus residence time at different temperatures. Reaction conditions: P_t = 2 bar, O_2/CH_4 ratio = 15, and mole fraction of Argon = 90%.

Moreover, results show that by increasing O_2/CH_4 ratio, formaldehyde yield increases while temperature variation does not play any noticeable roles. Therefore, it seems that the best-operating conditions are high O_2/CH_4 ratio and any temperature in the acceptable range of LTO. However, one can argue that at low temperatures, see Figures 9 to 11, formaldehyde formation zone in the microreactor spreads out which is helpful for controlling the process in term of withdrawing formaldehyde. Therefore operating conditions would favor low temperature and high O_2/CH_4 ratio. Also, it should be noted at maximum formaldehyde yield, its selectivity is less than 100% which means the existence of by-products. Also, carbon monoxide, carbon dioxide, hydrogen, water, and C_2 hydrocarbons are the main by-products with traces of other chemicals.

Design Criteria

Residence time depends on reactor volume and feed flow rate. However, at any operating conditions of temperature and O_2/CH_4 ratio, the residence time must be determined in a way to guarantee the production of formaldehyde at the output of microreactor. This is possible with reference to Figures 9 to 11. For example in Figure 11, the residence time operating microreactor at T = 1000 K and O_2/CH_4 = 15 should be 522 ms in order to produce maximum yield (amount) of formaldehyde. Residence time corresponding to the maximum yield of formaldehyde at microreactor output depends on O_2/CH_4 and temperature. It can be seen that maximum yield does not change with temperature which implies that residence time corresponding to maximum yield of formaldehyde at the output is a function of O_2/CH_4 ratio only. It should be noted that the temperature change along the reactor length is negligible, as shown in Figure 12, and could be assumed that the temperature is almost constant during the time of reaction.

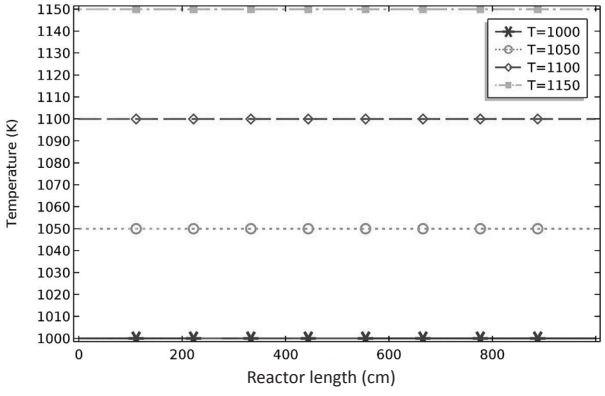

Figure 12: Temperature variation versus reactor length at different temperatures. Reaction conditions: P_t = 2 bar, τ = 30 ms, O_2/CH_4 ratio = 15, and mole fraction of Argon = 90%.

It can be noticed that an annular microreactor allows very rapid heating and cooling of components, and leads to a relatively constant temperature [33]. Figures 13 shows residence time and yield as functions of O_2/CH_4 ratio at temperature of 1000 K. The maximum yield of formaldehyde can be reached up to 5.5% per single pass of microreactor system in the residence time of 493 ms which corresponds with the optimum operating condition (T = 1000 K and O_2/CH_4 ratio = 17).

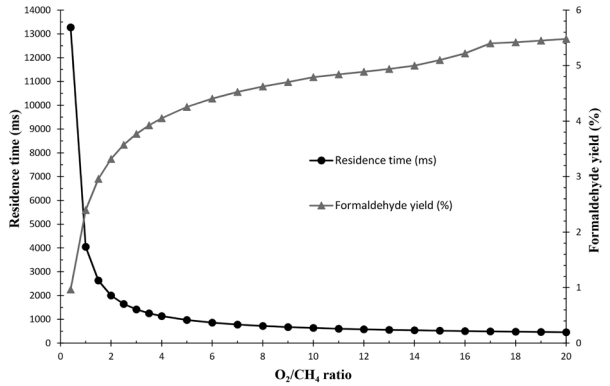

Figure 13: Residence time and formaldehyde yield as a function of O_2/CH_4 ratio. Reaction conditions: P_t = 2 bar, T = 1000 K, and mole fraction of Argon = 90%.

CONCLUSIONS

Pathways for production of formaldehyde from LTO of methane were analyzed, modeled, and confirmed by available experimental data. It is found out that increasing temperature beyond 1000 K does not affect formaldehyde yield, and it is O_2/CH_4 ratio which is an influential parameter to increase yield and to determine the residence time in microreactor to guarantee formaldehyde production at the output of microreactor system. Moreover, it is concluded that the maximum yield of formaldehyde by LTO of methane can be reached up to 5.5% per single pass in a microreactor system. Finally, the production of by-products is inevitable under all conditions, and efforts are needed to reduce them.

NOMENCLATURES

F_i	: Molar flow rate of species i, mol/s
C_i	: Concentration of species i, mol/m^3
C_{i0}	: Initial concentration of species i, mol/m^3
C^{in}_i	: Inlet concentration of species i, mol/m^3
T	: Reactor temperature, K
T^{in}	: Reactor temperature, K
P_t	: Reactor pressure, bar
V	: Reactor volume, m^3
L	: Reactor Length, m
D	: Reactor diameter, m
R_i	: Reaction rate of species i, mol/m^3/s
r_j	: Reaction rate of reaction j, mol/m^3/s
H_j	: Enthalpy of the reaction j, J/mol
$Q_{heat\ source}$	: Heat of reactions, J/m^3/s
Q_{ext}	: External heat added or removed the reactor, J/m^3/s
q_{cond}	: Conductive heat transfer, W
N_i	: Molar flux of component i, mol/m^2/s
z	: Axial coordinate, m
t	: Times, s
A_C	: Cross sectional area, m^2
E	: Activation energy, J/mol
$D_{i,mix}$	: The diffusivity coefficient in mixture, m^2/s
Re	: Reynolds number
Sc	: Schmidt number
Pe_{MT}	: Peclet number for mass transfer
$K_j(T)$	: The kinetic rate constant for reaction j with units of (volume/mole)$^{nj-1}$/time
n_j	: The simplified order of the j-th reaction
R^*_j	: Dimensionless rate law for the j-th reaction

Greek Letters

υ_{ij}	: Stoichiometric coefficient of species i in reaction j
Λ^2_{ij}	: Damkohler number for component i in the j-th chemical reaction

REFERENCES

1. Zakaria Z. and Kamarudin S. K., "Direct Conversion Technologies of Methane to Methanol: An Overview," *Renewable and Sustainable Energy Reviews*, **2016**, *65*, 250-261.
2. Holmen A., "Direct Conversion of Methane to fuels and Chemicals," *Catalysis Today*, **2009**, *142*(1), 2-8.

3. Nasr J. and Abrishami A., "Energy Management and Process Improvement of Methanol Production," *Journal of Petroleum Science and Technology*, **2012**, *2*(2), 33-39.
4. Maklavany D. M., Shariati A., Khosravi-Nikou M. R., and Roozbehani B., "Hydrogen Production via Low Temperature Water Gas Shift Reaction: Kinetic Study," Mathematical Modeling, Simulation and Optimization of Catalytic Fixed Bed Reactor using gPROMS. Chemical Product and Process Modeling, **2017**, *12*(3), 3-23.
5. Ghodoosi F., Khosravi-Nikou M. R., and Shariati A., "Mathematical Modeling of Reverse Water-Gas Shift Reaction in a Fixed-Bed Reactor," *Chemical Engineering and Technology*, **2017**, *40*(3), 598-607.
6. Zhang J., Burklé-Vitzthum V., and Marquaire P., "NO 2-promoted Oxidation of Methane to Formaldehyde at Very Short Residence Time–Part II: Kinetic Modeling," *Chemical Engineering Journal*, **2012,** *197*, 123-134.
7. Arutyunov V., "Low-scale Direct Methane to Methanol-Modern Status and Future Prospects," *Catalysis Today*, **2013**, *215*, 243-250.
8. Zhang Q., He D., and Zhu Q., "Recent Progress in Direct Partial Oxidation of Methane to Methanol," *Journal of Natural Gas Chemistry*, **2003**, *12*(2), 81-89.
9. Koo K., "Autothermal Reforming of Methane to Syngas for Fischer–Tropsch Synthesis with Promoted Palladium and a Fast Start-up Device," *Research on Chemical Intermediates*, **2008**, *34*(8), 803-810.
10. Moshrefi M. M., Rashidi F., and Bozorgzadeh H. R., "Use of a DC Discharge in a Plasma Reactor with a Rotating Ground Electrode for Production of Synthesis Gas by Partial Oxidation of Methane," *Research on Chemical Intermediates*, **2015**, *41*(9), 5941-5959.
11. Foulds, G. and B. Gray, "Homogeneous Gas-phase Partial Oxidation of Methane to Methanol and Formaldehyde," *Fuel Processing Technology*, **1995**, *42*(2), 129-150.
12. Thomas D. J., Willi R., and Baiker A., "Partial Oxidation of Methane: the Role of Surface Reactions," *Industrial and Engineering Chemistry Research Journal*, **1992**, *31*(10), 2272-2278.
13. Zhang J., "Direct Conversion of Methane in Formaldehyde at Very Short Residence Time," *Chemical Engineering Science*, **2011**, *66*(24), 6331-6340.
14. Benlounes O., "Direct Oxidation of Methane to Oxygenates over Heteropolyanions," *Journal of Natural Gas Chemistry*, **2008**, *17*(3), 309-312.
15. De Vekki A. and Marakaev S., "Catalytic Partial Oxidation of Methane to Formaldehyde," *Russian Journal of Applied Chemistry*, **2009**, *82*(4), 521-536.
16. Wang Y., "Selective Oxidation of Hydrocarbons Catalyzed by Iron-containing Heterogeneous Catalysts," *Research on Chemical Intermediates*, **2006**, *32*(3), 235-251.
17. Jun J. H., Lee T. J., Lim T. H., Nam S. W., et al., "Nickel-calcium Phosphate/hydroxyapatite Catalysts for Partial Oxidation of Methane to Syngas: Effect of Composition," *Korean Journal of Chemical Engineering*, **2004**, *21*(1), 140-146.
18. Liu Z. W., Roh H. S., Jun K. W., Park S. E., and Song T. Y., "Partial Oxidation of Methane over Ni/Ce-Zro_2/θ-Al_2O_3," *Korean Journal of Chemical Engineering*, **2002**, *19*(5), 742-748.
19. Liu Z. W., Jun K. W., Roh H. S., Park S. E., and Oh

Y. S., "Partial Oxidation of Methane over Nickel Catalysts Supported on Various Aluminas," *Korean Journal of Chemical Engineering*, **2002**, *19*(5), 735-741.

20. Han Z. S., "Preparation and Effect of Mo-V-Cr-Bi-Si Oxide Catalysts on Controlled Oxidation of Methane to Methanol and Formaldehyde," *Korean Journal of Chemical Engineering*, **1998**, *15*(5), 496-499.
21. Bozorgzadeh H. R., "Catalytic and Non-catalytic Conversion of Methane to C_2 Hydrocarbons in a Low Temperature Plasma," *Journal of Petroleum Science and Technology*, **2015**, *5*(1), 69-78.
22. Tabata K., "Activation of Methane by Oxygen and Nitrogen Oxides," *Catalysis Reviews*, **2002**, *44*(1), 1-58.
23. Görke O., Pfeifer P., and Schubert K., "Highly Selective Methanation by the Use of a Microchannel Reactor," *Catalysis today*, **2005**, *110*(1), 132-139.
24. Michalkiewicz B., "Partial Oxidation of Methane to Formaldehyde and Methanol Using Molecular Oxygen over Fe-ZSM-5," *Applied Catalysis A: General*, **2004**, *277*(1–2), 147-153.
25. Duan C., Luo M., and Xing X., "High-rate Conversion of Methane to Methanol by Methylosinus trichosporium OB3b," *Bioresource Technology*, **2011**, *102*(15), 7349-7353.
26. Lee S. G. , "Optimization of Methanol Biosynthesis from Methane using Methylosinus Trichosporium OB3b," *Biotechnology Letters*, **2004**, *26*(11), 947-950.
27. Villa K., Murcia-López S., Andreu T., and Morante J. R., "Mesoporous WO3 Photocatalyst for the Partial Oxidation of Methane to Methanol Using Electron Scavengers," *Applied Catalysis B: Environmental*, **2015**, *163*, 150-155.
28. Rodríguez-Guerra Y., Gerling L. A., López-Guajardo E. A., Lozano-García F. J., and et al., "Design of Micro- and Milli-Channel Heat Exchanger Reactors for Homogeneous Exothermic Reactions in the Laminar Regime," *Industrial and Engineering Chemistry Research*, **2016**, *55*(22), 6435-6442.
29. Kshetrimayum K. S., "CFD Simulation of Microchannel Reactor Block for Fischer–Tropsch Synthesis: Effect of Coolant Type and Wall Boiling Condition on Reactor Temperature," *Industrial and Engineering Chemistry Research Journal*, **2016**, *55*(3), 543-554.
30. Anxionnaz Z., "Heat Exchanger/reactors (HEX Reactors): Concepts, Technologies: State-of-the-art," *Chemical Engineering and Processing: Process Intensification*, **2008**, *47*(12), 2029-2050.
31. Kristal J., "Practical Engineering Aspects of Catalysis in Microreactors," *Research on Chemical Intermediates*, **2015**, *41*(12), 9357-9371.
32. Su M., "Synthesis of Highly Monodisperse Silica Nanoparticles in the Microreactor System," *Korean Journal of Chemical Engineering*, **2017,** *34*(2), 484-494.
33. Burkle-Vitzthum V., "Annular Flow Microreactor: An Efficient Tool for Kinetic Studies in Gas Phase at very Short Residence Times," *Chemical Engineering Research and Design*, **2015**, *94*, 611-623.
34. Frenklach M., Bowman C. T., Smith G. P., and Gardiner W. C., "World Wide Web location http://www. me. berkeley. edu. gri_mech," Version **1999**, 3(0).
35. Balaji S. and Lakshminarayanan S., "Improved Design of Microchannel Plate Geometry for

Uniform Flow Distribution," *The Canadian Journal of Chemical Engineering*, **2006**, *84*(6), 715-721.

36. Commenge J., "Optimal Design for Flow Uniformity in Microchannel Reactors", *AIChE Journal*, **2002**, *48*(2), 345-358.
37. Bird R. B., Stewart W. E., and Lightfoot E. N., "Transport Phenomena (2nd ed.)," *John Wiley and Sons*, **2007**, 1-897.
38. Belfiore L. A., Way J. J., and Zhang L., "Transport Phenomena for Chemical Reactor Design (1st ed.)," *Kirk-Othmer Encyclopedia of Chemical Technology*, **2000**, 1-865.
39. Glarborg P., "PSR: A FORTRAN Program for Modeling Well-stirred Reactors," *Sandia Report SAND86-8209*, **1986**.
40. Alam F. E., "Influence of Trace Nitrogen Oxides on Natural Gas Oxidation: Flow Reactor Measurements and Kinetic Modeling," *Journal of Energy and Fuels,* **2016**, *31*(3), 2360-2369.
41. Da Silva M. J., "Synthesis of Methanol from Methane: Challenges and Advances on the Multi-step (Syngas) and One-step Routes (DMTM)," *Fuel Processing Technology Journal*, **2016**, *145*, 42-61.
42. Rasmussen C. L., Jakobsen J. G., and Glarborg P., "Experimental Measurements and Kinetic Modeling of CH_4/O_2 and $CH_4/C_2H_6/O_2$ Conversion at High Pressure," *International Journal of Chemical Kinetics*, **2008**, *40*(12), 778-807.
43. Aasberg-Petersen K., Hansen J. H. B., Christensen T. S., Dybkjaer I., Christensen P. and et al., "Technologies for Large-scale Gas Conversion," *Applied Catalysis A: General,* **2001**, *221*(1), 379-387.